Supplementary Materials

Understanding Charge Transport and Recombination in High Performance Polymer Solar Cells with Non-Fullerene Acceptors

Xuning Zhang, Xiaobing Zuo, Shenkun Xie, Jianyu Yuan,* Huiqiong Zhou,* and Yuan Zhang*

Materials & methods

Materials: PBDB-T, ITIC and $PC_{71}BM$ were purchased from Solarmer, Inc (Beijing) and P(NDI2OD-T2) was from 1-Material, Inc (Quebec, Canada). All materials were used as received without additional purification.

Device Fabrication: For solar cells fabrication, ITO (indium-tin-oxide) coated glass substrates were cleaned with detergent solution by scrubbing and sonicated sequentially in ultra-pure water (18 MΩ), acetone, and iso-propanol and dried before use. The hole transport layer in solar cells was attained by spin-coating PEDOT:PSS (Al 4083, H.C. Starck) solution on UV-zone treated ITO/glass substrates at 3000 rpm for 40 s (thickness ~40 nm). PBDB-T:ITIC (1:1 weight ratio) was solubilized in chlorobenzene:DIO solution (99.5:0.5 volume ratio) with a total concentration of 20 mg/mL, PBDB-T:P(NDI2OD-T2) (1:1 weight ratio) was solubilized in chlorobenzene:DIO (99.5:0.5 volume ratio) with a total concentration of 8 mg/mL, and PBDB-T: $PC_{71}BM$ (1:1 weight ratio) was solubilized in chlorobenzene:DIO (97:3 volume ratio) with a total concentration of 20 mg/mL. Photoactive layers were attained by spin-casting the BHJ solutions at appropriate spin rates, leading to an optimal thickness around 100 nm. Finally, 10 nm of Ca and 100 nm of Al protection layer were thermally evaporated on top on the BHJ layer through shadow masks in a vacuum < 10^{-7} Torr. For single-carrier devices, the active layers were prepared identically to the procedure for solar cells. In hole-only devices, the top electron-blocking contact was fabricated by thermally depositing 80 nm of Au. For electron-only devices, 30 nm of Al bottom contact was deposited atop pre-cleaned glass substrates, followed by spin-coating the BHJ solutions. Finally the top Ca/Al cathode was deposited similarly as for solar cells. To reduce the leakage current, strip-shaped ITO were used which were patterned through etching, leading to an effective device area 0.04 cm^2.

Characterization: The film thickness of solar cells and single carrier devices were determined by a surface profilometer (KLA Tencor D-120).The transmittance and absorbance spectra were attained by using a UV-Vis spectrometer (Perkin Elmer Lambda 650/850/950 UV-Vis spectrophotometer). Current density-voltage (*J-V*) characteristics of solar cells were measured using a Keithley 2400 source meter under AM 1.5 G illumination (100 mW/cm^2) provided by an Oriel solar simulator. The incident light intensity was adjusted with a silicon calibration photodiode (Peccell Technologies). The IPCE spectra were registered by using a solar cell spectral response measurement system (QER3011, Enli Technology Co. Ltd). Single carrier devices were characterized in a Lakeshore vacuum probe station by a Keithley 4200 semiconductor parameter analyzer in dark environment. Low temperature (215-295 K) was realized by purging liquid nitrogen into the vacuum chamber controlled by a Lakeshore temperature controller. *J-V* characteristics of single carrier devices were fitted manually by using the OriginPro 8.5 data analysis software. The GIWAXS measurements were performed at Beamline 12-ID-B of the Advanced Photon Source (APS) at Argonne National Laboratory. The X-ray energy was 14 keV and the incident angle was set at ca. 0.1^{o} to maximize the scattering intensity. The scattered X-rays were measured using a Perkin Elmer detector, XRpad 4343F.

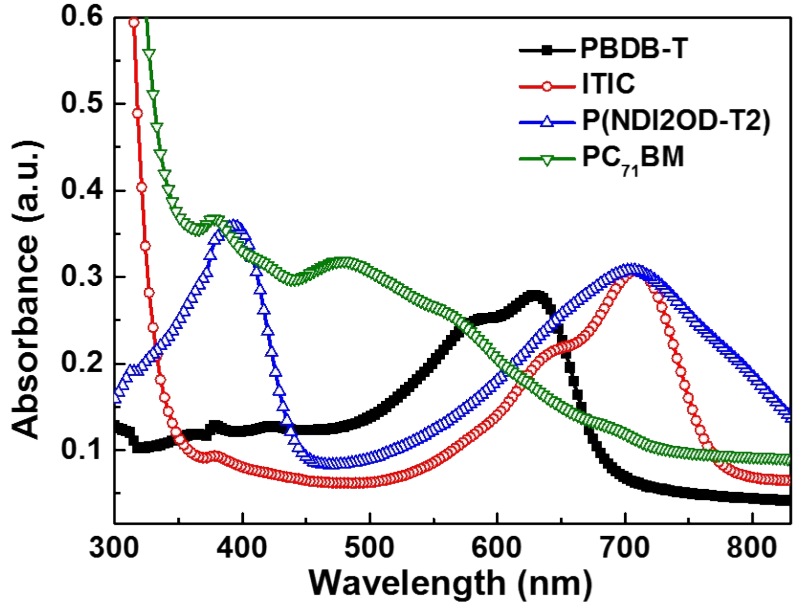

Fig. S1. Thin film absorption of pristine PBDB-T donor and ITIC, P(NDI2OD-T2), and $PC_{71}BM$ acceptors.

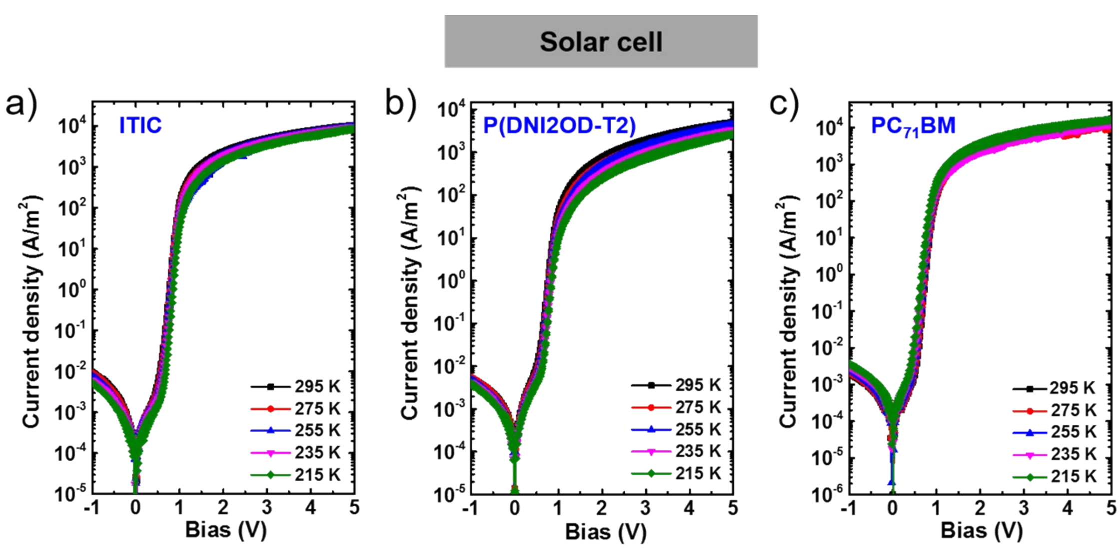

Fig. S2. *T*-dependent dark *J-V* characteristics of solar cells based on BHJs comprised of (a) PBDB-T:ITIC, (b) PBDB-T:P(NDI2OD-T2), and (c) PBDB-T:$PC_{71}BM$.

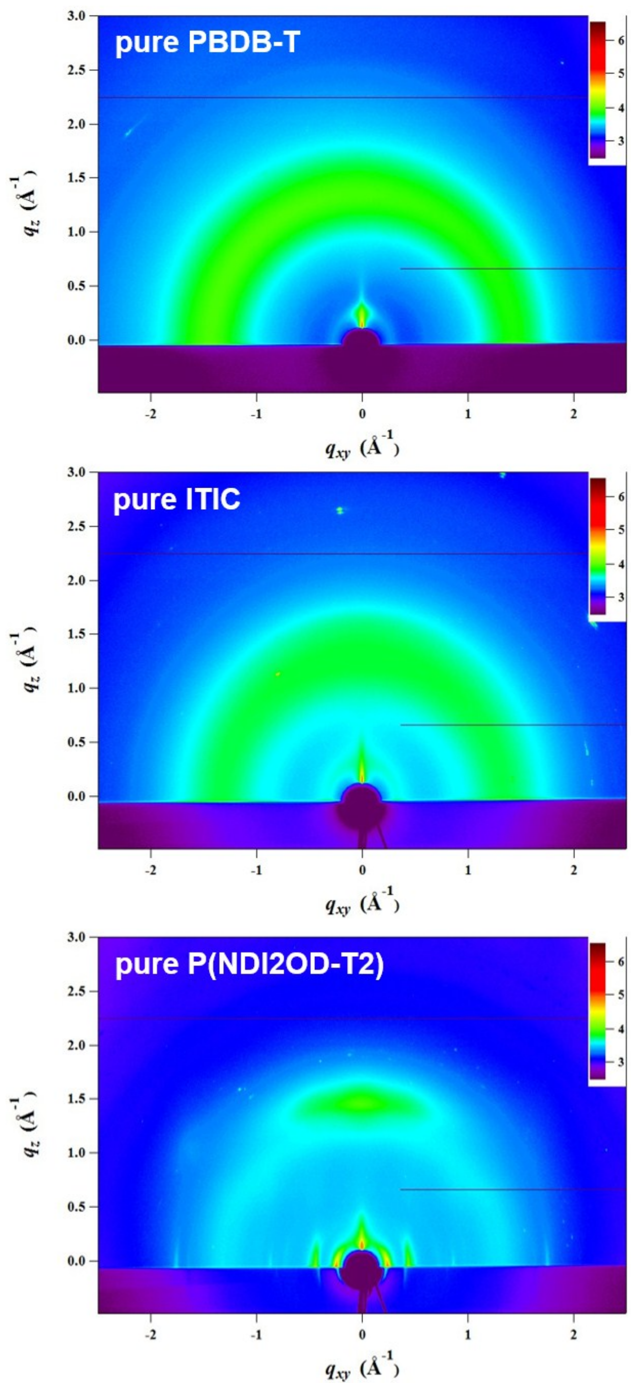

Fig. S3. 2D images of GIWAXS patterns for pristine PBDB-T and non-fullerene ITIC and P(NDI2OD-T2) acceptors used in this study.

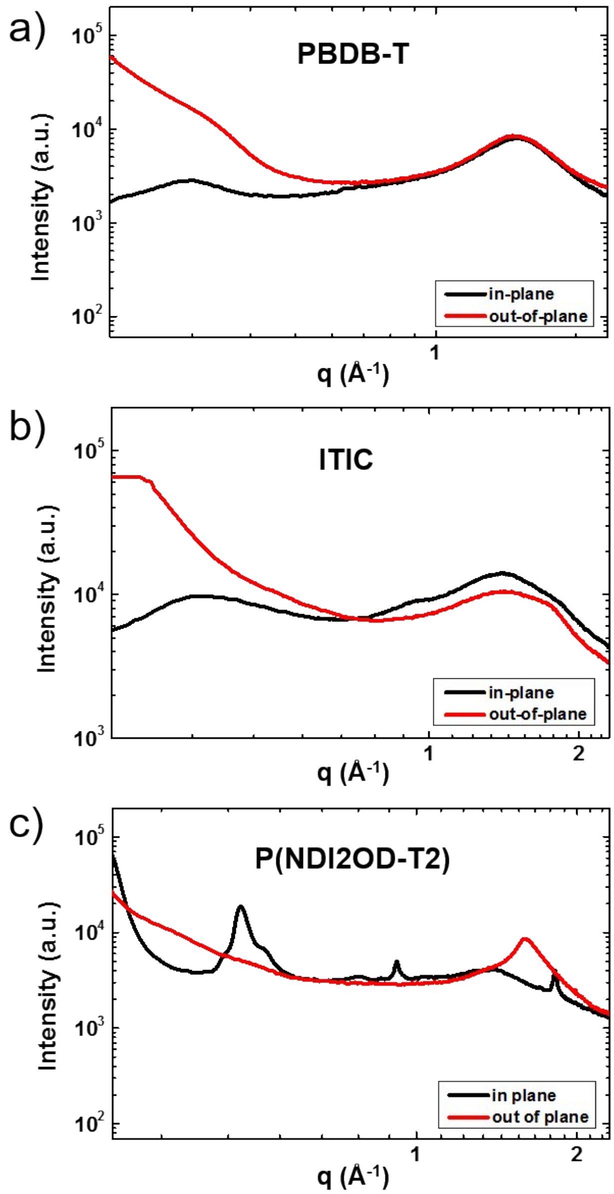

Fig. S4. 1D patterns of out-of-plane and in-plane line cut from GIWAXS patterns of pristine (a) PBDB-T, (b) ITIC, and (c) P(NDI2OD-T2).

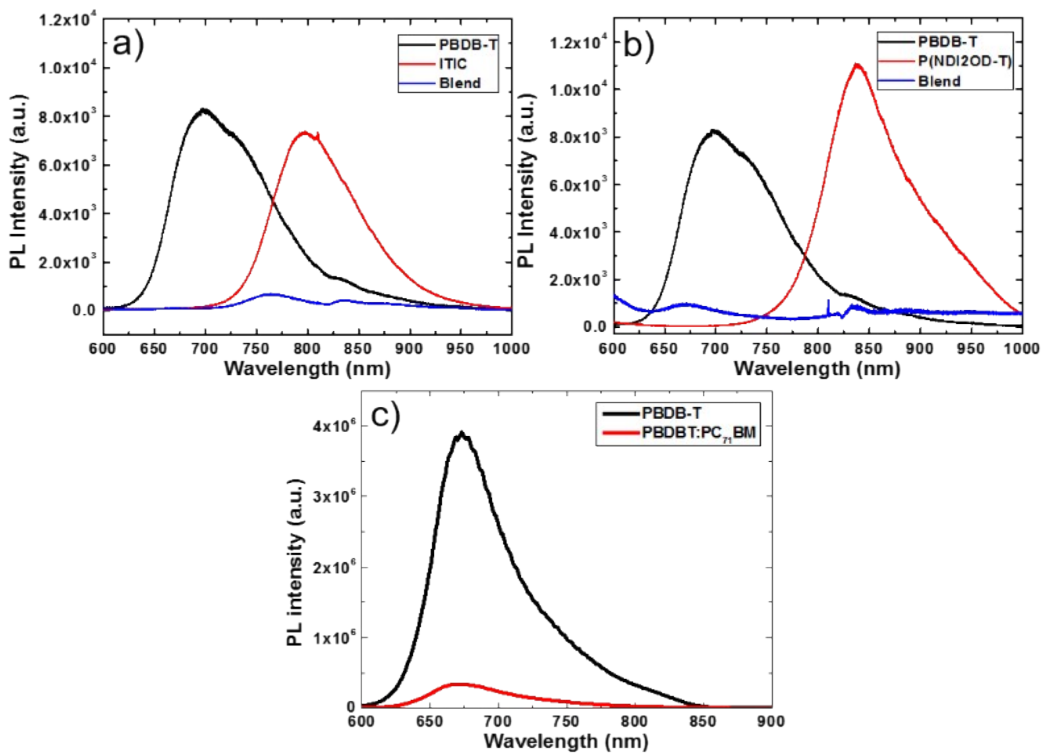

Fig. S5. Photoluminescence spectra of thin films based on (a) neat PBDB-T, ITIC, and PBDB-T:ITIC blend, (b) neat PBDB-T, P(NDI2OD-T), and PBDB-T:P(NDI2OD-T) blend, and (c) neat PBDB-T and PBDB-T:$PC_{71}BM$ blend.

Table S1. Solar cell parameters based on conventional device architecture measured under 1.5 AM G irradiation (100 mW/cm^2).

Acceptor	V_{oc} (V)	J_{sc} (mA/cm^2)	FF (%)	PCE (%)
ITIC	0.90	15.8[a] (15.8)[b]	68.4	9.7
P(NDI2OD-T2)	0.88	8.4[a] (8.3)[b]	70.0	5.6
$PC_{71}BM$	0.83	11.4[a] (11.2)[b]	72.4	7.4

[a] Values based on *J-V* characteristics of solar cells under 1 sun.
[b] Values in parenthesis are based integration from IPCE spectra.

Table S2. SCLC mobility of single-carrier devices and solar cells at different *T* determined by fittings using Mott-Gurney law based on various BHJs in this study (mobility unit in m^2/Vs).

Acceptor	Temperature (K)	Electron-only	Hole-only	Solar cell
ITIC	295	1.75E-09	1.06E-07	1.26E-07
	275	1.30E-09	5.84E-08	6.64E-08
	255	7.36E-10	3.17E-08	6.16E-08
	235	4.57E-10	1.89E-08	4.81E-08
	215	2.97E-10	1.25E-08	2.99E-08
P(NDI2OD-T2)	295	2.01E-08	3.98E-08	6.25E-08
	275	1.81E-08	2.99E-08	5.73E-08
	255	1.49E-08	2.28E-08	5.26E-08
	235	1.12E-08	1.12E-08	4.95E-08
	215	1.00E-08	8.56E-09	4.65E-08
$PC_{71}BM$	295	1.02E-07	5.82E-08	3.10E-07
	275	1.17E-07	4.82E-08	2.96E-07
	255	6.38E-08	2.59E-08	2.32E-07
	235	3.84E-08	1.92E-08	1.42E-07
	215	2.42E-08	8.32E-09	1.82E-07